CONFIDENTIAL. Limited circulation. For review only.

# Supercapacitor stability and control for More Electric Aircraft application

Antonio Russo, Alberto Cavallo

***Abstract*— This paper deals with the stability analysis and the control of a supercapacitor in the framework of the More Electric Aircraft (MEA). The objective is to reduce the stress on the mechanical part of the aeronautic power generator caused by the typical piece-wise constant current profile of the Electro-Mechanical Actuators (EMAs) onboard the aircraft. Stability properties of the open-loop system are proven through a rigorous theoretical analysis aimed at demonstrating the stability uniformly with any arbitrarily chosen switching signal. The control strategy considered is a Second Order Sliding Mode, able to guarantee monotonic convergence of the sliding variable to the origin. Detailed simulations have been provided in order to verify the effectiveness of the proposed control strategy.**

## I. Introduction

In the last decade great importance has been devoted to the implementation of devices and technologies leading to the the realization of the MEA [1], [2]. In brief, the idea is to replace hydraulic and/or pneumatic actuators with the more reliable electric ones, e.g., EMAs (Electro-Mechanical Actuators) or EHAs (Electro Hydrostatic Actuators) [3] to actuate mobile control surfaces [4]. In [5] different locations (e.g., flaps, air brakes, landing gears) for electrically driven actuators onboard a commercial aircraft are reviewed, along with technologic advancement required for the MEA. The European Community has funded many research projects on the topic, with the objective to reduce weight and emissions, e.g., to reduce pollution, within the CleanSky and CleanSky2 initiatives [6] and the incoming CleanSky3 [7], aimed to cut 80% of air transport CO2 emissions by 2050. In addition to control actuation, three more areas where the MEA concept can result in appreciable benefits have been pointed out, namely internal engine starter/generator, integrated (auxiliary and emergency) power unit, and fault tolerant power management [8]. It is currently accepted in the aeronautic community that the MEA approach results into new technological challenges. For instance, the selection of different electric motor solutions for different applications (landing gears, aeronautic surfaces, electric pumps) has been investigated [9]. It is also clear that the increased number of electric devices onboard requires the development of more complex automatic control strategies, and simple approaches based on linear controllers with stability proofs based on local linearization are no longer sufficient.

This work was partially supported by CleanSky2 grant Programme: H2020-CS2-CFP06-2017-01 JTI-CS2-2017-CFP06-REG-01-10 Proposal: 785416 ENIGMA

The authors are with Department of Engineering, University of Campania, 81031 Aversa, Italy {antonio.russo1, alberto.cavallo}@unicampania.it

The use of advanced devices, such as supercapacitors, is of great interest for the management of electric energy onboard, and will be addressed in this paper. Supercapacitors can be employed as "fast" storage devices (faster than traditional batteries) and they can be used to reduce fatigue on the aircraft generator by smoothing the power requests to the generator itself [10]. In other words, if a load (such as an EMA) requires a fast power delivery, a supercapacitor can provide a peaky power profile, allowing the generator to supply the (smooth) remaining part. Similarly, if the power request suddenly decreases, the supercapacitor must absorb a peaky power profile [11]. This is accomplished through controlled converter placed between the supercapacitor and the electric network. This also allows to interface the different levels of voltage of the network (typically 270V) and the supercapacitor (typically around 100V). The controller must guarantee that the supercapacitor supplies power to the EMA when needed, but stability issues must also be taken into account. In spite of the passive nature of the components of the network, it is not difficult to provide counter-examples showing that even for a power grid with passive elements, in the presence of controlled devices (such as the EMA), unstable behavior may occur. In [12] it has been shown that a CPL (constant power load) can be synthesized using switching converters driven by a sliding mode control algorithm. A small-signal analysis shows that CPL's may have destabilising effect on the overall network [13], [14] since they have locally *negative resistances* [15]. Note however that a CPL is just an idealization of the reality, since there is no load that can absorb (or supply) infinite current at zero voltage. In order to assess the stability of the electric network, a rigorous alternative to the small-signals approximation is to use the Input-to-State Stability (ISS) approach [16], which is a stability property known for providing a bound on the state norm related to the magnitude of the inputs.

It must be noted that this work presents several improvements compared to a previous work of the same authors [11]. In fact, a more precise stability analysis, based on the definition of ISS, is proposed here and a different controller, which reaches a suitably defined sliding manifold without overshoot, has been adopted in this work.

To the best of authors' knowledge, this is the first paper where the ISS approach is used in the MEA context, as opposed to the standard local stability analysis after linearization. The result is sensible from a physical point of view and produces a quantitative estimate of the norm of the system state, along with the decay rate.

Manuscript 204 submitted to 2020 European Control Conference.
Uploaded October 23, 2019.

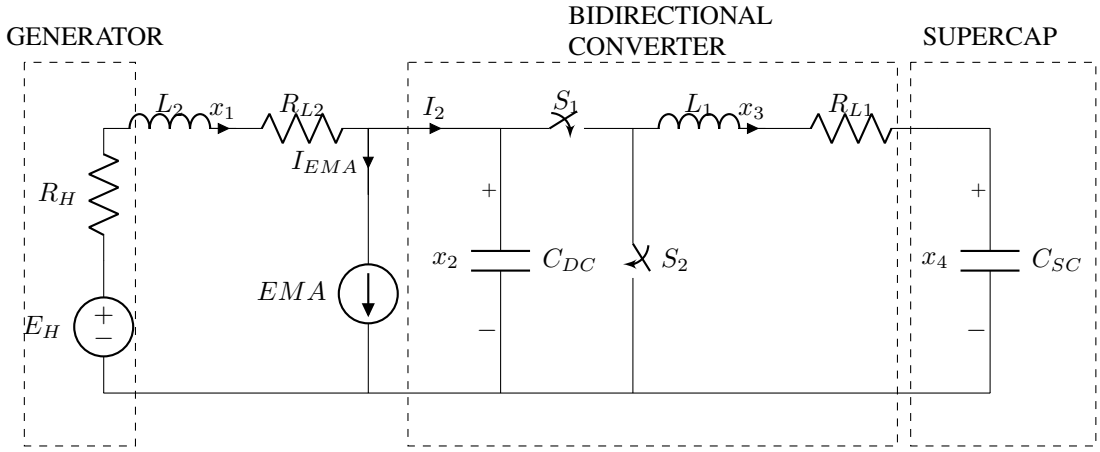


Fig. 1: Bidirectional converter schematic

## II. The Mathematical Model

### A. Notation

For the sake of notation, we define here the following [17]: a function $\alpha : \mathbb{R}_{\geq 0} \to \mathbb{R}_{\geq 0}$ is *positive definite* if it is continuous, $\alpha(r) > 0 \quad \forall r > 0$ and $\alpha(0) = 0$; it is of class $\mathcal{K}$ if it is positive definite and is strictly increasing; it is of class $\mathcal{K}_\infty$ if it is a class $\mathcal{K}$ function and also $\alpha(r) \to \infty$ as $r \to \infty$; it is of class $\mathcal{L}$ if it is continuous, strictly decreasing and $\alpha(r) \to 0$ as $r \to \infty$. A function $\beta : \mathbb{R}_{\geq 0} \times \mathbb{R}_{\geq 0} \to \mathbb{R}_{\geq 0}$ is a class $\mathcal{KL}$ function if for each fixed $t$, the function $\beta(s,t)$ is a class $\mathcal{K}$ function with respect to $s$, and for each fixed $s$ the function $\beta(s,t)$ is of class $\mathcal{L}$ with respect to $t$. Given a function $p(t)$ we will denote with $|p(t)|$ the standard Euclidean norm and $\|p\|_\infty \coloneqq ess\sup\{|p(s)|, s \in \mathbb{R}_{\geq 0}\}$. Finally, given two matrices $A$ and $B$, $A \otimes B$ indicates the Kronecker product between $A$ and $B$, while $vec(A)$ vectorizes the matrix $A$.

### B. The Electrical Power Grid

The network schematic, reported in Figure 1, shows the electric grid subject of this work. From left to right, $E_H$ represents the $270V$ voltage generator with inner resistance $R_H$. The generator is connected to the rest of the grid through an electric bus modeled as a transmission line with lumped inductance $L_2$ and resistance $R_{L2}$. The Electro-Mechanical Actuator is here modeled as a controlled current source, while the bidirectional converter comprises of the following elements: two switches working in counter-phase, namely $S_1$ and $S_2$, a capacitor with capacitance $C_{DC}$, an inductor $L_1$ and a resistor $R_{L1}$. Finally, the supercapacitor is here modeled as a large capacitor of capacitance $C_{SC}$.

Considering the two possible configurations of the switches (namely, $S_1$ on, $S_2$ off and $S_1$ off, $S_2$ on), it is trivial to retrieve the system equations which can be collected in the form of a bilinear system

$$\begin{aligned}\dot{x} &= \begin{bmatrix} -\frac{R_{L_2}+R_H}{L_2} & -\frac{1}{L_2} & 0 & 0 \\ \frac{1}{C_{DC}} & 0 & 0 & 0 \\ 0 & 0 & -\frac{R_{L_1}}{L_1} & -\frac{1}{L_1} \\ 0 & 0 & \frac{1}{C_{SC}} & 0 \end{bmatrix} x \\ &+ \begin{bmatrix} 0 & 0 & 0 & 0 \\ 0 & 0 & -\frac{1}{C_{DC}} & 0 \\ 0 & \frac{1}{L_1} & 0 & 0 \\ 0 & 0 & 0 & 0 \end{bmatrix} xu + \begin{bmatrix} \frac{E_H}{L_2} \\ -\frac{I_{EMA}(t)}{C_{DC}} \\ 0 \\ 0 \end{bmatrix} \\ &= Ax + Bxu + \Gamma(t), \end{aligned} \tag{1}$$

where $u \in \{0,1\}$, $x \coloneqq [x_1,\ x_2,\ x_3,\ x_4]^T$ with $x_1$ being the generator current flowing through the inductor $L_2$, $x_2$ is the voltage on the capacitor $C_{DC}$, $x_3$ is the current flowing through the inductor $L_1$ and $x_4$ is the supercapacitor voltage. Finally, we indicate with $I_{EMA}$ the current flowing through the EMA, while $I_2$ is the current entering the bidirectional converter that can be trivially obtained applying Kirchhoff's current law and resulting in

$$I_2 = x_1 - I_{EMA}. \tag{2}$$

Moreover, in the rest of the paper we will assume that $I_{EMA}(t)$ is bounded and we will denote with $\Gamma_{\max} \coloneqq \|\Gamma(t)\|_\infty$.

## III. Stability Properties of the System

In the following it will be formally proven that system (1) cannot undergo any unstable behavior for any switching signal arbitrarily chosen.

Since $u \in \{0,1\}$, system (1) can be equivalently represented as a switched linear system in the form

$$\dot{x} = A_i x + \Gamma(t), \qquad \text{with} \quad i \in \{0,1\} \tag{3}$$

with $A_0 = A$ and $A_1 = A + B$. In what follows we will prove some properties related to the stability of system (1).

*Lemma 1:* Consider the system (1) and the associated switched system

$$\dot{z} = A_i z, \qquad \text{with} \quad i \in \{0,1\} \tag{4}$$

and $A_0 = A$ and $A_1 = A + B$. Then matrices $A_0$ and $A_1$ are Hurwitz and the switched system (4) shares a common quadratic Lyapunov function $V(z) = z^T P z$ with $P$ being the symmetric positive definite solution of the Lyapunov equations

$$A_0^T P + P A_0 = -Q_0, \tag{5}$$
$$A_1^T P + P A_1 = -Q_1, \tag{6}$$

with $Q_0$ diagonal and $Q_1$ symmetric being positive definite matrices suitably chosen.

*Proof:* The proof of this Lemma is constructive and is provided in the Appendix. ∎

Given the existence of a common quadratic Lyapunov function for the switched system (4), it is possible to demonstrate that the ISS property holds for system (1) uniformly for any arbitrarily chosen switching signal $u(t)$. This is proven in the next Theorem. Let us preliminarily present a result from [16] that is here given as the definition of ISS in terms of Lyapunov function.

*Definition 1 (ISS):* The system $\dot{x}(t) = f(x(t), d(t))$ with $x \in \mathbb{R}^n$, $d \in \mathbb{R}^m$ is said to be ISS if and only if there exists a smooth function $V : \mathbb{R}^n \to \mathbb{R}_{\geq 0}$ such that there exist functions $\alpha_1$, $\alpha_2$, $\alpha_3 \in \mathcal{K}_\infty$, and a function $\chi \in \mathcal{K}$ such that the following holds

$$\alpha_1(|x|) \leq V(x) \leq \alpha_2(|x|), \tag{7}$$
$$\nabla V(x) \cdot f(x, u) \leq -\alpha_3(|x|) + \chi(|d|). \tag{8}$$

for all $x \in \mathbb{R}^n$ and $d \in \mathbb{R}^m$.

It is now possible to characterize the ISS property of the system (1) by using the following Theorem.

*Theorem 1:* The switched system (3) is ISS with respect to $\Gamma(t)$ for any arbitrary switching, with a decay rate equal to $\frac{3}{4}\frac{\eta}{\lambda_{\max}(P)}$ with $\eta \coloneqq \min\{\lambda_{\min}(Q_0), \lambda_{\min}(Q_1)\}$ and $P$ being a symmetric positive definite matrix such that equality (5) and (6) hold for two positive definite matrices $Q_0$ and $Q_1$. Moreover, $V(x) = x^T P x$ is a quadratic ISS Lyapunov function for the system.

*Proof:* Lemma 1 proves that the subsystems of the switched system (4) share a common quadratic Lyapunov function $V(x) = x^T P x$ with $P$ being the symmetric positive definite matrix such that (5) and (6) are satisfied simultaneously. Then, let us consider a candidate ISS Lyapunov function as

$$V(x) = x^T P x. \tag{9}$$

Its time derivative is

$$\begin{aligned} \dot{V}(x) &= \dot{x}^T P x + x^T P \dot{x}, \\ &= (A_i x + \Gamma(t))^T P x + x^T P (A_i x + \Gamma(t)), \\ &= x^T (A_i^T P + P A_i) x + 2\Gamma^T(t) P x, \\ &\leq \eta \left( -|x|^2 + \frac{2}{\eta} |\Gamma^T(t) P| |x| \right), \end{aligned} \tag{10}$$

Consider now the property $2ab \leq a^2 + b^2$ and choose $a = |x|/2$ and $b = \frac{2}{\eta}|\Gamma^T P|$, then

$$\dot{V}(x) \leq -\frac{3}{4}\eta |x|^2 + \frac{4}{\eta}\lambda_{\max}^2(P) |\Gamma_{\max}|^2. \tag{11}$$

We just obtained a $\dot{V}(x)$ in the form (8), then the open-loop system (1) is ISS for any arbitrary switching. Moreover, note that, from (9) it holds $|x|^2 \geq V/\lambda_{\max}(P)$, hence, replacing this in (11) it results in

$$\dot{V} \leq -\frac{3}{4}\frac{\eta}{\lambda_{\max}(P)} V + \frac{4}{\eta}\lambda_{\max}^2(P) |\Gamma_{\max}|^2. \tag{12}$$

∎

In the scope of the specific application of this work, the generator voltage $E_H$ is assumed to be a known constant while the profile of $I_{EMA}(t)$ is supposed to be unknown. Hence, it is of higher interest to investigate the stability properties of system (1) with respect to $I_{EMA}(t)$ instead of the entire vector $\Gamma(t)$. Next definition, from [18], is useful for the characterization of the system stability properties with respect to $I_{EMA}$.

*Definition 2 (ISpS):* The system $\dot{x}(t) = f(x(t), d(t))$ with $x \in \mathbb{R}^n$, $d \in \mathbb{R}^m$ is said to be Input-to-State practically Stable (ISpS) if there exist a function $\beta$ of class $\mathcal{KL}$, a function $\gamma$ of class $\mathcal{K}$ and a nonnegative constant $c$ such that it hold

$$|x(t)| \leq \beta(|x(t_0)|, t - t_0) + \gamma(||d||_\infty) + c, \tag{13}$$

for any $x(t_0) \in \mathbb{R}^n$ and $d \in \mathbb{R}^m$ and all $t \geq t_0 \geq 0$.

*Corollary 1:* The system (1) is ISpS with respect to $I_{EMA}(t)$ for any arbitrary switching.

*Proof:* The proof follows from similar considerations presented in Theorem 1 and is here omitted for the sake of brevity. ∎

## IV. System Controller

The main objective of the controller is to exploit the presence of the supercapacitor to smoothen the generator current when the EMA requires a piece-wise varying current. In fact, the supercapacitor is called for providing the "fast" transient component of the current required by the EMA while the "slow" transient component and the steady state component are provided by the generator. Referring to Figure 1, a time varying current reference $\hat{I}_2(t)$ can be selected by filtering the EMA current through a high-pass filter, i.e.

$$\hat{I}_2(t) = D(t) * I_{EMA}(t) \tag{14}$$

where the operator $*$ denotes the convolution, and $D(t)$ is the impulse response of the filter. In order to formally state the current control problem for the supercapacitor control, the following sliding variable can be introduced.

$$\sigma(t, x) = x_3 x_4 - x_2 \hat{I}_2(t). \tag{15}$$

By regarding the sliding variable in (15) as relevant system outputs, it appears that its relative degree (i.e., the minimum order $r$ of the time derivative $\sigma^{(r)}$ in which the control $u$ explicitly appears) is equal to one. Hence, a first order sliding mode control could in theory be implemented to control this system. However, in practical implementation, a PWM modulator with fixed frequency is used. Therefore, the control law that drives the PWM signal generator cannot be discontinuous, which implies that a first order sliding

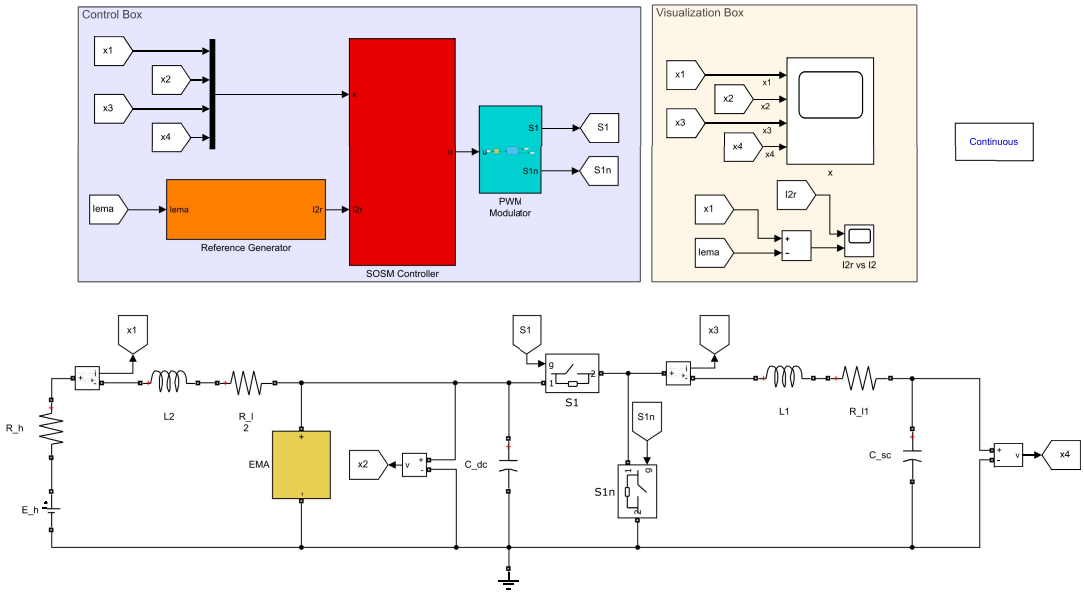


Fig. 2: SimPowerSystem Simulation Scheme

mode control is not admissible in this application. This also implies that the control input $u$ is no longer a binary variable with values in the set $\{0, 1\}$, but it must be considered as a continuous signal with values in the interval $[0, 1]$. For the sake of simplicity, the same symbol $u$ will be used for both cases, since there is no possibility of misunderstanding. A possible solution to obtain a continuous control is to artificially increase the relative degree of the system and to resort to a Second Order Sliding Mode (SOSM). According to the Suboptimal SOSM control theory [19], we can define the auxiliary system as

$$\begin{aligned} \dot{\xi}_1(t) &= \xi_2(t), && (16)\\ \dot{\xi}_2(t) &= f(x,t) + g(x,t)w, && (17)\\ \dot{u} &= w, && (18) \end{aligned}$$

where $\xi_1(t) = \sigma(t)$, $f(x,t)$ and $g(x,t)$ are uncertain bounded vector fields assumed bounded by virtue of the results from the ISS analysis of the Section III. Hence it is possible to assume

$$\begin{aligned} |f(x,t)| &\leq F, && (19)\\ 0 < G_1 \leq g(x,t) &\leq G_2, && (20) \end{aligned}$$

where $F$, $G_1$ and $G_2$ quantify the uncertainty of the vector fields. Define positive scalars $\delta$, $M$ and $\kappa^*$ such that

$$\left.\begin{array}{l} \delta \in [0,1) \\ M > \frac{F}{G_1} \\ \kappa^* \in [1;+\infty) \bigcap \left[\frac{F+(1-\delta)G_2 M}{\delta G_1 M}; +\infty\right) \end{array}\right\}. \quad (21)$$

Then the following theorem can be stated.

*Theorem 2:* Consider the system (1) and the auxiliary system (16)–(18) with uncertain dynamics bounded as in (19) and (20). Assume that the sequence of extremal values of $\sigma(t)$, $\sigma_{t_k} = \sigma(t_k)$ (i.e. the value of $\sigma$ at the last time instant at which $\dot{\sigma}(t) = 0$) is known. Then, the control strategy

$$w(t) = -\kappa(t) M \text{sign}(\sigma - \sigma_{t_k}), \quad (22)$$

where

$$\kappa(t) = \begin{cases} 1 & \text{if } (\sigma(t) - \delta\sigma_{t_k})\,\sigma_{t_k} \geq 0 \\ \kappa^* & \text{if } (\sigma(t) - \delta\sigma_{t_k})\,\sigma_{t_k} < 0 \end{cases} \quad (23)$$

and parameters $\kappa^*$, $\delta$ and $M$ are selected as in (21), causes the finite time *monotonic* convergence of $\sigma$ and $\dot{\sigma}$ to the origin of the plane $(\sigma, \dot{\sigma})$ and the stability of the closed-loop system.

*Proof:* It is not difficult to show that system (1),(16)–(18) has relative degree equal to two, hence SOSM techniques can be applied to obtain a smooth control action. Proof of the monotonic finite time convergence of the sliding function and its time derivative to the origin of the state plane follows directly from [20]. Once on the manifold, the stability of the zero dynamics directly follows from the result of Theorem 1. ■

## V. Simulation Results

The proposed SOSM control and associated strategy for the peaks smoothing algorithm have been tested in a detailed MATLAB/Simulink/SimPowerSystem simulator, shown in Figure 2, and composed of three blocks:

- Reference Generator: implements the logic for the generation of $\hat{I}_2(t)$ as in (14), with transfer function $D(s) = s\tau/(1 + s\tau)$ (orange block);
- SOSM Controller: contains the SOSM controller as presented in Section IV (red block);
- PWM Modulator: contains the modulator that implements the switching logic (cyan block).

The system and controller parameters are shown respectively in Table Ia and Table Ib where $\nu$ is the PWM modulator fixed

| Parameter | Value | |
|---|---|---|
| $E_H$ | 270 | [V] |
| $R_H$ | 100 | [mΩ] |
| $R_{L_1}$ | 89.2 | [mΩ] |
| $R_{L_2}$ | 10 | [mΩ] |
| $L_1$ | 24 | [$\mu$H] |
| $L_2$ | 2.4 | [$\mu$H] |
| $C_{DC}$ | 6 | [$\mu$F] |
| $C_{SC}$ | 7.95 | [F] |

(a) System Parameters

| Parameter | Value | |
|---|---|---|
| $\nu$ | 200 | [kHz] |
| $\delta$ | $10^{-3}$ | |
| $M$ | 5 | |
| $k^*$ | 2 | |
| $\tau$ | 1 | [s] |

(b) Controller Parameters

TABLE I: Simulation parameters

frequency and $\delta$, $M$ and $k^*$ are the controller parameters selected as shown in Section IV. The simulation has been designed using a realistic EMA current profile.

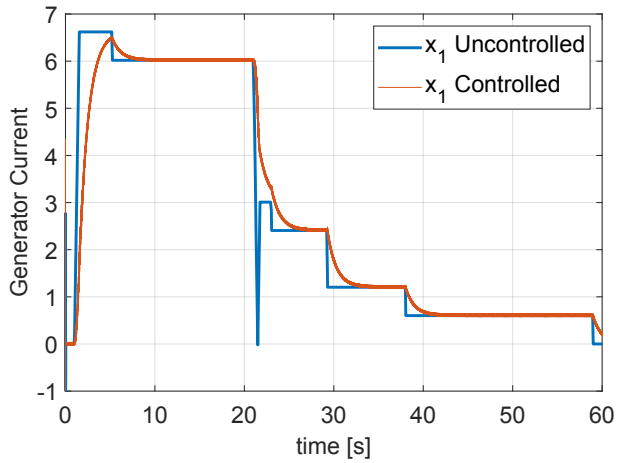


Fig. 3: Generator current: uncontrolled vs controlled behavior

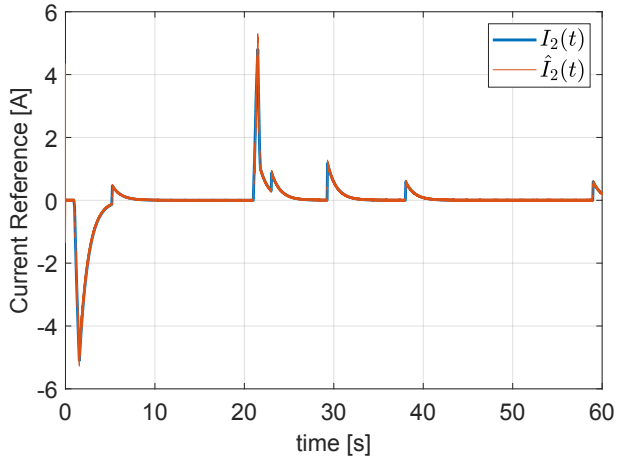


Fig. 4: Current $I_2(t)$ vs Reference Current $\hat{I}_2(t)$

Figure 3 shows the benefits of the controller action: the blue line represents the generator current when the control algorithm is inactive (which corresponds to the EMA current profile), while the red line, represents the generator current obtained when the control algorithm is active. As expected, the generator current affected by the action of the controlled supercapactior, results in a smoother profile. This in turns implies less stress on the mechanical part of the power generator. The current profile to be tracked by the controller, i.e. $\hat{I}_2(t)$, and the actual evolution of the current $I_2(t)$ are presented in Figure 4, which also denotes the good tracking performance achieved by the controller.

## VI. CONCLUSIONS

This paper presented the theoretical stability analysis and control of a supercapacitor based on SOSM for a MEA application. Specifically, a bidirectional converter is used to regulate the power flow between the power generator and a supercapacitor in order to implement a peaks smoothing action on the generator current. Proofs of ISS of the open-loop system are provided and the theoretical results are tested through a detailed simulator. Further results will move towards the definition of a more general procedure to verify the ISS property for electrical power grids.

## APPENDIX

In the following, the statement of Lemma 1 will be proven. For the sake of notation, let us rename the elements of matrices $A_0$ and $A_1$ with different symbols, i.e.

$$A_0 = \begin{bmatrix} -a & -b & 0 & 0 \\ c & 0 & 0 & 0 \\ 0 & 0 & -d & -e \\ 0 & 0 & f & 0 \end{bmatrix}, \quad A_1 = \begin{bmatrix} -a & -b & 0 & 0 \\ c & 0 & -c & 0 \\ 0 & e & -d & -e \\ 0 & 0 & f & 0 \end{bmatrix} \tag{24}$$

with $a, b, c, d, e, f$ being positive scalars such that $a = \frac{R_{L_2}+R_H}{L_2}$, $b = \frac{1}{L_2}$, $c = \frac{1}{C_{DC}}$, $d = \frac{R_{L_1}}{L_1}$, $e = \frac{1}{L_1}$ and $f = \frac{1}{C_{SC}}$. It is trivial to verify that the eigenvalues of $A_0$ are

$$\lambda_{1,2} = -\frac{1}{2}\left(a \pm \sqrt{a^2 - 4bc}\right) \tag{25}$$

$$\lambda_{3,4} = -\frac{1}{2}\left(d \pm \sqrt{d^2 - 4ef}\right) \tag{26}$$

which are all characterized by negative real part. For the matrix $A_1$, instead, using Routh method, it can be easily proven that $A_1$ is Hurwitz. Hence, both matrices $A_0$ and $A_1$ are Hurwitz for any positive choice of the scalars $a, b, c, d, e$ and $f$. In order to prove that the subsystems of the switched systems (4) share a common quadratic Lyapunov function, we must verify that there exists a symmetric positive definite matrix $P$ which simultaneously satisfies equality (5) and (6) for given positive matrices $Q_0$ and $Q_1$. Initially, let us choose $Q_0$ as

$$Q_0 = \begin{bmatrix} q_0 & 0 & 0 & 0 \\ 0 & q_1 & 0 & 0 \\ 0 & 0 & q_2 & 0 \\ 0 & 0 & 0 & q_3 \end{bmatrix} \tag{27}$$

with $q_0, q_1, q_2$ and $q_3$ being positive scalars. Matrix $Q_0$ is obviously positive definite while $P$ can be calculated

from (5) as

$$G = \left(A_0^T \otimes I\right) + \left(I \otimes A_0^T\right), \tag{28}$$
$$Gvec(P) = -vec(Q_0). \tag{29}$$

This results in $P$ being

$$P = \begin{bmatrix} \frac{bq_0+cq_1}{2ab} & \frac{q_1}{2b} & 0 & 0 \\ \frac{q_1}{2b} & \frac{q_1\left(a^2+bc\right)+q_0b^2}{2abc} & 0 & 0 \\ 0 & 0 & \frac{eq_2+fq_3}{2de} & \frac{q_3}{2e} \\ 0 & 0 & \frac{q_3}{2e} & \frac{q_3\left(d^2+fe\right)+q_2e^2}{2def} \end{bmatrix}. \tag{30}$$

Using Sylvester's criterion it becomes easy to verify positive definiteness of matrix $P$ uniformly for any arbitrary values of the parameters. Let us now consider $Q_1 = -(A_1^T P + P A_1)$,

$$Q_1 = \begin{bmatrix} q_0 & 0 & \frac{c}{2b}q_1 & 0 \\ 0 & q_1 & \theta & -\frac{q_3}{2} \\ \frac{c}{2b}q_1 & \theta & q_2 & 0 \\ 0 & -\frac{q_3}{2} & 0 & q_3 \end{bmatrix} \tag{31}$$

with $\theta = \frac{b^2q_0+(a^2+bc)q_1}{2ab} - \frac{eq_2+fq_3}{2de}$. Note that $Q_1$ is symmetric, thus Sylvester's criterion is applicable. The four leading principal minors of $Q_1$ are

$$\begin{aligned} \psi_1 &= q_0, \\ \psi_2 &= q_0q_1, \\ \psi_3 &= q_1\left(q_0q_2 - \frac{c^2}{4b^2}q_1^2\right) - \theta^2q_0, \\ \psi_4 &= q_3\left(q_0q_2 - \frac{c^2}{4b^2}q_1^2\right)\left(q_1 - \frac{q_3}{4}\right) - \theta^2q_0q_3. \end{aligned}$$

It follows that some conditions are needed for the parameters $q_0, q_1, q_2$ and $q_3$ in order to guarantee $\psi_3 > 0$ and $\psi_4 > 0$ simultaneously. Let us choose $q_2$ such that $\theta = 0$, i.e

$$\begin{aligned} q_2 &= \frac{1}{abe}\left(b^2dq_0 + d\left(a^2+bc\right)q_1 - abfq_3\right) \\ &= k_0q_0 + k_1q_1 - k_3q_3, \end{aligned} \tag{32}$$

with $k_0 \coloneqq db/ae, k_1 \coloneqq \frac{d(a^2+bc)}{abe}$ and $k_3 \coloneqq f/e$. Note that this recalls the need to impose an upper bound on $q_3$ in order to guarantee the positiveness of $q_2$, that is

$$q_3 < \frac{k_0q_0 + k_1q_1}{k_3}. \tag{33}$$

Let us now consider $\psi_4$. In order for it to be positive, it is sufficient to have

$$q_0 > \frac{c^2}{4b^2}\frac{q_1^2}{q_2}, \tag{34}$$
$$q_3 < 4q_1. \tag{35}$$

hence, eventually choosing $q_3$ such that $q_3 < \min\left\{4q_1, \frac{k_0q_0+k_1q_1}{k_3}\right\}$ will fulfill the positiveness of $\psi_4$. Note that condition (34), together with the choice of $q_2$ as in (32), guarantees the positive definiteness of $\psi_3$. Moreover, from (32) and (34) we obtain

$$k_0q_0^2 + (k_1q_1 - k_3q_3)q_0 - \frac{c^2}{4b^2}q_1^2 > 0, \tag{36}$$

and using (35)

$$k_0q_0^2 + (k_1 - 4k_3)q_1q_0 - \frac{c^2}{4b^2}q_1^2 > 0. \tag{37}$$

Note that it is always possible to find a $q_0$ such that (37) is satisfied. Hence, it is always possible to find a positive definite matrix $P$ that satisfies (5) and (6) using the following procedure:

1) Select positive $q_1$ freely,
2) Select positive $q_0$ that satisfies (37),
3) Select positive $q_3 < \min\left\{4q_1, \frac{k_0q_0+k_1q_1}{k_3}\right\}$,
4) Select positive $q_2 = k_0q_0 + k_1q_1 - k_3q_3$.

## REFERENCES


[1] [Online]. Available: www.moreelectricaircraft.com

[2] J. A. Rosero, J. A. Ortega, E. Aldabas, and L. Romeral, "Moving towards a more electric aircraft," *IEEE Aerospace and Electronic Systems Magazine*, vol. 22, pp. 3–9, 2007.

[3] M. A. Maldonado, N. M. Shah, K. J. Cleek, P. S. Walia, and G. Korba, "Power management and distribution system for a more-electric aircraft (madmel)-program status," in *IECEC 96. Proceedings of the 31st Intersociety Energy Conversion Engineering Conference*, vol. 1, Aug 1996, pp. 148–153 vol.1.

[4] (2006-2009) Moet-more open electrical technologies. [Online]. Available: http://ec.europa.eu/research/transport/projects/items/moet_en.htm

[5] G. Qiao, G. Liu, Z. Shi, Y. Wang, S. Ma, and T. C. Lim, "A review of electromechanical actuators for more/all electric aircraft systems," *Proceedings of the Institution of Mechanical Engineers, Part C: Journal of Mechanical Engineering Science*, vol. 232, no. 22, pp. 4128–4151, 2018. [Online]. Available: https://doi.org/10.1177/0954406217749869

[6] (2010-2015) Clean sky at a glance. [Online]. Available: http://www.cleansky.eu/content/document/clean-sky-glance-0

[7] (2020-2025) Aeronautics industry proposal for clean sky 3 programme. [Online]. Available: https://www.asd-europe.org/aeronautics-industry-proposal-for-clean-sky-3-programme

[8] R. T. Naayagi, "A review of more electric aircraft technology," in *2013 International Conference on Energy Efficient Technologies for Sustainability*, April 2013, pp. 750–753.

[9] W. Cao, B. C. Mecrow, G. J. Atkinson, J. W. Bennett, and D. J. Atkinson, "Overview of electric motor technologies used for more electric aircraft (mea)," *IEEE Transactions on Industrial Electronics*, vol. 59, no. 9, pp. 3523–3531, Sep. 2012.

[10] R. Todd, D. Wu, J. Dos Santos Girio, M. Poucand, and A. Forsyth, "Supercapacitor-based energy management for future aircraft systems," in *Conference Proceedings - IEEE Applied Power Electronics Conference and Exposition - APEC—Conf Proc IEEE Appl Power Electron Conf Expo APEC*, 2010, pp. 1306–1312.

[11] A. Cavallo, A. Russo, and G. Canciello, "Control of supercapacitors for smooth EMA operations in aeronautical applications," in *2019 American Control Conference (ACC)*, July 2019, pp. 4948–4954.

[12] B. A. Martínez-Treviño, A. E. Aroudi, and L. Martínez-Salamero, "Synthesis of constant power loads using switching converters under sliding mode control," in *2018 IEEE International Symposium on Circuits and Systems (ISCAS)*, May 2018, pp. 1–5.

[13] A. B. Jusoh, "The instability effect of constant power loads," in *PECon 2004. Proceedings. National Power and Energy Conference, 2004.*, Nov 2004, pp. 175–179.

[14] A. Griffo and J. Wang, "Large signal stability analysis of 'more electric' aircraft power systems with constant power loads," *IEEE Transactions on Aerospace and Electronic Systems*, vol. 48, no. 1, pp. 477–489, Jan 2012.

[15] A. Emadi, A. Khaligh, C. H. Rivetta, and G. A. Williamson, "Constant power loads and negative impedance instability in automotive systems: definition, modeling, stability, and control of power electronic converters and motor drives," *IEEE Transactions on Vehicular Technology*, vol. 55, no. 4, pp. 1112–1125, July 2006.

[16] E. D. Sontag and Yuan Wang, "New characterizations of input-to-state stability," *IEEE Transactions on Automatic Control*, vol. 41, no. 9, pp. 1283–1294, Sep. 1996.

[17] H. Khalil, *Nonlinear Systems*, ser. Pearson Education. Prentice Hall, 2002. [Online]. Available: https://books.google.com/books?id=t_d1QgAACAAJ

[18] Z. P. Jiang, A. R. Teel, and L. Praly, "Small-gain theorem for iss systems and applications," *Mathematics of Control, Signals and Systems*, vol. 7, no. 2, pp. 95–120, Jun 1994. [Online]. Available: https://doi.org/10.1007/BF01211469

[19] G. Bartolini, A. Ferrara, and E. Usai, "Applications of a sub-optimal discontinuous control algorithm for uncertain second order systems," *International Journal of Robust and Nonlinear Control*, vol. 7, pp. 299 – 319, 04 1997.

[20] G. Bartolini, A. Pisano, E. Punta, and E. Usai, "A survey of applications of second-order sliding mode control to mechanical systems," *International Journal of Control*, vol. 76, no. 9-10, pp. 875–892, 2003. [Online]. Available: https://doi.org/10.1080/0020717031000099010